Empirically Adopted IEM for Retrieval of Soil Moisture From Radar Backscattering Coefficients

Kaijun Song, Xiaobing Zhou, and Yong Fan, *Member, IEEE*

***Abstract*—The integral equation model (IEM) is considered as a promising algorithm for soil moisture retrieval from active microwave data over bare soil and sparsely vegetated conditions. However, the soil dielectric constant is implicitly embedded in the complicated IEM; inversion of soil moisture is often accomplished through iteration and is thus computationally expensive, particularly when it is applied to retrieve soil moisture from active microwave data on a large scale. To simplify the inversion process of soil moisture directly from the active microwave data, basic math functions were adopted to fit the simulation results of the original IEM so that the radar backscattering coefficient becomes an explicit function of soil dielectric constant or the soil dielectric constant is an explicit function of radar backscattering coefficient. Soil moisture is then calculated directly from radar backscattering coefficient without iteration. We called this model empirically adopted IEM (EA-IEM). The accuracy of the EA-IEM to the original IEM and its applicability are analyzed through three processes: model intercomparison, sensitivity analysis, and model comparison with *in situ* measurements. The average differences of backscattering coefficients between the EA-IEM and the original IEM are 0.14 dB for HH-polarization and 0.12 dB (Gaussian correlation function) and 0.2 dB (exponential correlation function) for VV-polarization. The sensitivity of soil moisture variation is examined under the consideration of absolute and relative calibration errors. A comparison between the soil moisture estimated and the measurements is performed, and the root-mean-square (rms) error is found to be 3.4%, suggesting that the EA-IEM performs well in these real cases. All these analyses indicate that the EA-IEM is a good representative of the original IEM and can be used to retrieve soil moisture under the tested range of model parameters: incidence angles between 10° and 60°, soil dielectric constants between 4 and 42, surface rms height from 4 to 31 mm, and correlation length from 50 to 250 mm.**

***Index Terms*—Backscattering coefficient, empirically adopted integral equation model (EA-IEM), IEM, soil moisture.**

Manuscript received May 8, 2008; revised July 8, 2008, September 5, 2008, September 22, 2008, and October 26, 2008. First published March 16, 2009; current version published May 22, 2009. This work was supported in part by NASA through the Montana Space Grant Consortium (G316-06-W0381), by the Research Seed Grant of Montana Tech of The University of Montana, and by the Youth Science and Technology Foundation of the University of Electronic Science and Technology of China (JX0711).

K. Song was with the Department of Geophysical Engineering, Montana Tech of the University of Montana, Butte, MT 59701 USA. He is now with the School of Electronic Engineering, University of Electronic Science and Technology of China, 610054 Chengdu, China (e-mail: kjsong@ee.uestc.edu.cn).

X. Zhou is with the Department of Geophysical Engineering, Montana Tech of the University of Montana, Butte, MT 59701 USA (e-mail: xzhou@mtech.edu).

Y. Fan is with the School of Electronic Engineering, University of Electronic Science and Technology of China, 610054 Chengdu, China (e-mail: yfan@uestc.edu.cn).

Digital Object Identifier 10.1109/TGRS.2008.2009061

I. Introduction

SOIL MOISTURE content plays a critical role in the interaction between the land surface and the atmosphere and can be considered as a key state variable that influences the distribution of both shortwave solar energy and longwave radiant energy, the runoff generation, and the percolation of water into the soil. Therefore, the capacity of measuring soil moisture content on a large scale from space is very attractive. It is well known that active microwave remote sensing techniques have the capabilities of all-weather and night-and-day measurement, and the radar backscattering coefficient is sensitive to soil moisture content and soil roughness. Thus, many studies and methods have been undertaken in radar remote sensing research in order to retrieve the soil moisture and surface roughness from radar backscattering coefficients [1]–[12]. Many models have been developed to retrieve soil moisture content [13]–[19]. However, it is rather difficult to determine the soil moisture directly from radar backscattering coefficients without the inversion process.

Many empirical and semiempirical models have been developed to establish the relationships between synthetic aperture radar (SAR) backscattering coefficient with soil moisture and surface roughness. In some studies [13]–[15], the empirical models derived from *in situ* data sets can fit their data well. These empirical models may be very suitable under similar soil surface conditions and SAR system parameters as those on which the empirical models were developed. However, empirical models cannot usually be extrapolated to other regions because not all parameters are incorporated in the models. Due to the sensing configuration of active microwave systems, the representative surface power spectrum of the surface roughness correlation function and correlation length parameters are difficult to derive from either remote sensing techniques or *in situ* measurements. Therefore, these parameters are not usually taken into account in the empirical models.

Analytical electromagnetic backscattering models such as the physical optics (PO) model, the geometrical optics (GO) model, and the first-order small perturbation model (SPM) [19] have been developed to retrieve soil moisture from active microwave measurements. However, the SPM and PO models have been derived using some specific assumptions and therefore have a limited applicability in terms of surface roughness conditions. The integral equation model (IEM) developed by Fung *et al.* [17] offers a promising alternative approach for the retrieval of soil moisture and surface roughness from active microwave data since the model is valid for a wider range of surface roughness conditions when compared to other earlier

theoretical models [13], [16]. However, the IEM contains soil surface roughness parameters such as surface root-mean-square (rms) height, surface power spectrum of the surface roughness correlation function, and correlation length; sensing configuration parameters such as frequency (or wavelength) and look angle (or incidence angle); and dielectric constant of the soil. Of all parameters in the IEM, the roughness-related parameters are often difficult to determine [20]–[23]. The complexity of this model and the implicit relationship between soil dielectric constant and active microwave data make it difficult to directly derive soil moisture and roughness parameters from the active microwave data measured from natural surfaces.

Thus, it is necessary to develop an inversion model that is simple but general and can be applied to a wide range of soil surface conditions to derive soil moisture from active microwave data. The objective of this paper is to empirically adopt the IEM so that retrieving the soil surface moisture content from active microwave data can be directly performed and thus computationally efficient. The adoption is to be based on the original IEM, with the effect of surface power spectrum being included. Through nonlinear regression analysis, the empirically adopted IEM (EA-IEM) will be derived from fitting the model equations to numerical simulations from the original IEM under a wide range of soil dielectric constants, incidence angles, and surface roughness conditions. The EA-IEM will then be compared with *in situ* measurements (see Section V) to assess the general applicability of this model.

II. EA-IEM

A. Original IEM

The active microwave backscattering coefficient from a bare soil surface is a function of soil texture, structure, density, roughness (surface rms height), soil moisture, and soil surface conditions that are described by the autocorrelation function of random surface height and correlation length. For natural terrains that have a small rms slope, multiple scattering is not significant, and then, single scattering will dominate in most situations. Thus, copolarization backscattering coefficients are given by the IEM [17]

$$\sigma_{pp}^0 = \frac{k^2}{2}\exp\left(-2k_z^2\sigma^2\right)\sum_{n=1}^{\infty}\sigma^{2n}\left|I_{pp}^n\right|^2\frac{W^n(-2k_x,0)}{n!} \quad (1)$$

where $p = h$ (horizontal) or v (vertical) polarization and

$$I_{pp}^n = (2k_z)^n f_{pp}\exp\left(-k_z^2\sigma^2\right) + k_z^n\Phi_p(k_x)/2 \quad (2)$$

$$f_{vv} = \frac{2R_{\|}}{\cos\theta} \quad (3)$$

$$f_{hh} = -\frac{2R_{\perp}}{\cos\theta} \quad (4)$$

$$\Phi_v = F_{vv}(-k_x,0) + F_{vv}(k_x,0) = \frac{2\sin^2\theta(1+R_{\|})^2}{\cos\theta}\left[\left(1-\frac{1}{\varepsilon_r}\right) + \frac{\mu_r\varepsilon_r - \sin^2\theta - \varepsilon_r\cos^2\theta}{\varepsilon_r^2\cos^2\theta}\right] \quad (5)$$

$$\Phi_h = F_{hh}(-k_x,0) + F_{hh}(k_x,0) = -\frac{2\sin^2\theta(1+R_{\perp})^2}{\cos\theta}\left[\left(1-\frac{1}{\mu_r}\right) + \frac{\mu_r\varepsilon_r - \sin^2\theta - \mu_r\cos^2\theta}{\mu_r^2\cos^2\theta}\right] \quad (6)$$

where σ is the surface rms height, k is the wavenumber ($k = 2\rho/\lambda$, with λ being the wavelength of the radar signal), $k_z = k\cos\theta$, $k_x = k\sin\theta$, θ is the incidence angle, ε_r is the relative permittivity (relative dielectric constant) of the soil, μ_r is the relative permeability, and $R_{\|}$ and $R_{\perp}$ are the vertically and horizontally polarized Fresnel reflection coefficients, respectively. $W^n(k_x,k_y)$ is the Fourier transform of the nth power of a known surface correlation function which can be calculated by

$$W^n(k_x,k_y) = \frac{1}{2\pi}\iint\rho^n(x,y)\exp(jk_xx + jk_yy)dxdy \quad (7)$$

where $\rho(x,y)$ is the surface correlation function.

B. EA-IEM

Studies by Shi *et al.* [16] and Zribi and Dechambre [13] showed that the single-scattering IEM could be used to compute soil backscattering coefficients for bare soil or short-vegetated surfaces. However, application of the model to retrieve soil moisture from the active microwave backscattering coefficient is difficult because the dependence of the model on ε_r, θ, σ, surface power spectrum of the surface roughness correlation function, and correlation length is complicated and thus needs model inversion. Therefore, a new approach is desired to derive a direct inversion model that can be used to retrieve the soil dielectric constant directly from active microwave backscattering coefficients for bare soil or short-vegetated surfaces. Once the soil dielectric constant is retrieved from active microwave backscattering coefficients over bare soil surfaces, the soil moisture content can be found through applying empirical constant mixing models [24]–[26].

From (1)–(6), we can see that the dielectric constant ε_r only appears in I_{pp}^n that depends on both dielectric constant ε_r and incidence angle θ. To retrieve the soil dielectric constant, we have to invert ε_r from I_{pp}^n, which is usually difficult. Based on this observation, we can fit I_{pp}^n with suitable basic mathematical functions so that ε_r can be derived directly from the equations of backscattering coefficients.

To construct suitable functions for I_{pp}^n, we first analyze the ε_r dependence of f_{pp}/Φ_p. Fig. 1 shows f_{hh}/Φ_h versus dielectric constant ε_r at different incidence angles: $\theta = 30^\circ, 40^\circ$, and 50°. Results show that f_{hh}/Φ_h just changed by about 0.1 over a range of the dielectric constant from 4 to 42, which means that f_{hh}/Φ_h is very weakly dependent on the dielectric constant ε_r over the range of 4–42. Since both f_{hh} [(4)] and Φ_h [(5)] are explicit functions of ε_r, the weak dependence of f_{hh}/Φ_h means that the dependence of f_{hh} and Φ_h on the dielectric constant ε_r is almost the same. Based on this observation, we assume that both f_{hh} and Φ_h contain the same function that depends on ε_r. Thus, for HH-polarization, we define

$$f_{hh} = f_h(\varepsilon_r,\theta)f_{h1}(\theta) \quad (8)$$

$$\Phi_h = F_{hh}(-k_x,0) + F_{hh}(k_x,0) = 2f_h(\varepsilon_r,\theta)f_{h2}(\theta) \quad (9)$$

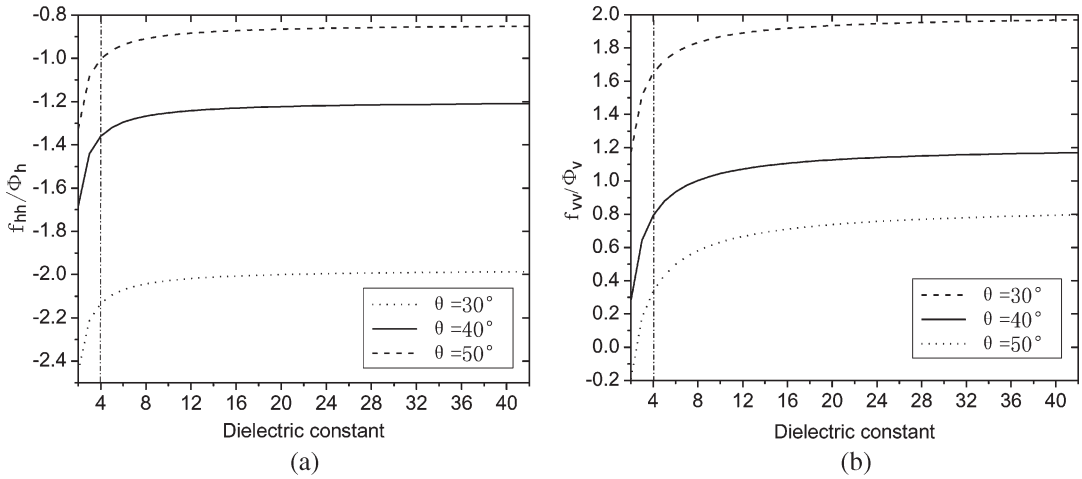

Fig. 1. ε_r dependence of f_{pp}/Φ_p for (a) HH-polarization and (b) VV-polarization.

where $F_h = f_h(\varepsilon_r, \theta)$ is a function of ε_r and θ. ε_r can be expressed explicitly as

$$\varepsilon_r = f_h^{-1}(F_h, \theta) \tag{10}$$

Then, I_{hh}^n can be expressed as

$$I_{hh}^n = f_h(\varepsilon_r, \theta) k_z^n \left[f_{h1}(\theta) 2^n \exp\left(-k_z^2 \sigma^2\right) + f_{h2}(\theta) \right]. \tag{11}$$

In (8)–(11), the specific forms of $f_h(\varepsilon_r, \theta)$, $f_{h1}(\theta)$, and $f_{h2}(\theta)$ are specified by fitting them to the simulation results of the original IEM, i.e., (4) and (6). Through nonlinear regression analysis using some basic mathematical functions, $f_h(\varepsilon_r, \theta)$, $f_{h1}(\theta)$, and $f_{h2}(\theta)$ are approximated as follows:

$$F_h = f_h(\varepsilon_r, \theta) = \frac{1.26(\varepsilon_r - 1.93)^{0.24\cos\theta}}{\sin^{3.94}\theta} \tag{12}$$

$$f_{h1}(\theta) = \frac{4175.4 \sin^{0.11}(\theta + 0.3) \sin^{3.91} 0.1\theta}{\sin^{0.86}(\theta + 1.5)} \tag{13}$$

$$f_{h2}(\theta) = -\frac{\sin^{5.9}\theta \sin^{0.22}(\theta + 0.5)}{\cos^{3.12} 0.8\theta} \tag{14}$$

where the incidence angle θ is in radians. The aforementioned formulas apply over a range of dielectric constant ε_r between 4 and 42 and incidence angle θ between 10° and 60°. For most geologic materials, ε_r lies within a range of 3–30, with dry sand at the lower end of this range at about 3–5. The range of 4–42 of dielectric constant covers the soil from very dry to wet regimes.

From (12), we derive the dielectric constant

$$\varepsilon_r = \left(\frac{F_h \sin^{3.94}\theta}{1.26} \right)^{4.167/\cos\theta} + 1.93 \tag{15}$$

where F_h is calculated from backscattering coefficient σ_{hh}^0 as follows:

$$F_h = \frac{\sqrt{2\sigma_{hh}^0} \exp\left(k_z^2 \sigma^2\right)/k}{\sqrt{\sum_{n=1}^{\infty} \left| f_{h1}(\theta) 2^n \exp(-2k_z^2\sigma^2) + f_{h2}(\theta) \right|^2 \frac{\sigma^{2n} k_z^{2n} W^n(-2k_x, 0)}{n!}}} \tag{16}$$

where $f_{h1}(\theta)$ can be calculated from (13) and $f_{h2}(\theta)$ from (14).

For the VV-polarization mode, we found that f_{vv}/Φ_v changed by about 0.4 (more than 50%) over the dielectric constant from 4 to 42 in Fig. 1(b), which means that the dependence of f_{vv}/Φ_v on the dielectric constant ε_r over the dielectric constant from 4 to 42 cannot be ignored. In other words, the dependence of f_{vv} and Φ_v on the dielectric constant ε_r is different. In this case, to secure accuracy, we adopt a different methodology than which was used for HH-polarization.

Let

$$I_{vv}^n = \sqrt{f_v(\varepsilon_r, \theta, \sigma, L)} (2k_z)^n \tag{17}$$

where $F_v = f_v(\varepsilon_r, \theta, \sigma, L)$ is a function of ε_r, θ, σ, and L. ε_r can be expressed as

$$\varepsilon_r = f_v^{-1}(F_v, \theta, \sigma, L). \tag{18}$$

Similarly, $f_v(\varepsilon_r, \theta, \sigma, L)$ is derived from a nonlinear regression analysis as (19a) and (19b), shown at the bottom of the page, for the Gaussian surface correlation function and the exponential surface correlation function, respectively. Here, the incidence angle θ is in radians, and the surface rms height σ and the surface correlation length L are in meters.

$$F_v = f_{vG}(\varepsilon_r, \theta, \sigma, L) = \frac{106 \left[0.5 - (\varepsilon_r + 3)^{-\cos(1.02\theta - 0.2)}\right]^{5.4} \exp\left(-1.996\sigma^2 k_z^2\right) \sigma^{-0.05}}{\sin^{3.35}(\theta + 1.1) \tan^{-0.46}(\theta + 0.32)(L - 0.049)^{[0.042 + 0.06\sin(\theta - 1)]}} \tag{19a}$$

$$F_v = f_{vE}(\varepsilon_r, \theta, \sigma, L) = \frac{\left[7 - (\varepsilon_r + 2.2)^{-\cos(0.98\theta - 0.2)}\right]^{81.61} \exp\left(-158.14 - 59.5\sigma - 1.8664\sigma^2 k_z^2\right)}{\exp\left[-2.31\tan(0.9\theta)\right] \sin^{2.1}(\theta + 0.77)(L - 0.046)^{[0.08 + 0.07\sin(\theta - 1.7)]}} \tag{19b}$$

Equations (19a) and (19b) apply over a range for the dielectric constant ε_r from 4 to 42, for the incidence angle θ from 10° to 60°, and for the surface rms height from 4 to 31 mm.

From (18), (19a), and (19b), we have dielectric constants (20a) and (20b), shown at the bottom of the page, for the Gaussian surface correlation function and the exponential surface correlation function, respectively. Here, F_v is calculated from the backscattering coefficient σ^0_{vv} for the dielectric constant retrieval as

$$F_v = \frac{\sigma^0_{vv}}{\frac{k^2}{2}\exp\left(-2k_z^2\sigma^2\right)\sum_{n=1}^{\infty}\frac{(2\sigma k_z)^{2n}W^n(-2k_x,0)}{n!}}. \tag{21}$$

III. Accuracy of the EA-IEM

From (12)–(14), (16), (19a), (19b), and (21), the horizontally and vertically copolarized backscattering coefficients are empirically adopted as (22) and (23a), shown at the bottom of the page, for the Gaussian surface correlation function and (23b), shown at the bottom of the page, for the exponential surface correlation function, respectively. These equations are functions of the local incidence angle θ (in radians), the dielectric constant ε_r, and the surface roughness parameters that include the surface rms height σ (in meters), the correlation length L (in meters), and the correlation functions $\rho(x,y)$, where θ is in radians and other parameters in SI units.

To assess the accuracy of the EA-IEM as compared with that of the original IEM, the horizontally and vertically copolarized backscattering coefficients (22)–(23b) are calculated under a range of soil moisture content and surface roughness conditions. Table I shows the ranges of dielectric constant, local incidence angle, surface rms height, correlation length, and sets of parameters as computation samples. Both the Gaussian function and the exponential function are chosen as the surface correlation functions.

TABLE I
Range of Parameters for Model Comparison

Model parameters	Minimum	Maximum	Interval	Unit
Dielectric constant	4	42	2	
Incidence angle	10	60	1	degree
RMS height	4	31	3	mm
Correlation length	50	250	25	mm
Correlation functions	Gaussian, exponential			

Fig. 2(a)–(c) shows the difference in decibels between the backscattering coefficients calculated by the original IEM [(1)] and by the EA-IEM [(22)–(23b)] for 5.3 GHz (C-band). From Fig. 2(a), it can be seen that the average difference between the original IEM and the EA-IEM is 0.14 dB for the HH-polarization backscattering coefficient; while for the VV-polarization backscattering coefficient, the differences are 0.12 and 0.2 dB, corresponding to the Gaussian and exponential surface correlation functions, as shown in Fig. 2(b) and (c), respectively. For the vertically copolarized backscattering coefficients σ^0_{vv}, the fit is good. Most of the computation samples, wherein the absolute difference between the original IEM and the EA-IEM exceeds 1 dB, occur at large incidence angle

$$\varepsilon_r = \frac{1}{\left(0.5 - \left(\frac{F_v\sigma^{0.05}\sin^{3.35}(\theta+1.1)(L-0.049)^{[0.042+0.06\sin(\theta-1)]}}{106\exp(-1.996\sigma^2k_z^2)\tan^{0.46}(\theta+0.32)}\right)^{5/27}\right)^{1/\cos(1.02\theta-0.2)}} - 3 \tag{20a}$$

$$\varepsilon_r = \frac{1}{\left(7 - \left(\frac{F_v\sin^{2.1}(\theta+0.77)(L-0.046)^{[0.08+0.07\sin(\theta-1.7)]}}{\exp[-158.14-59.5\sigma+2.31\tan(0.9\theta)-1.8664\sigma^2k_z^2]}\right)^{0.012253}\right)^{1/\cos(0.98\theta-0.2)}} - 2.2 \tag{20b}$$

$$\sigma^0_{hh} = \frac{0.7938k^2(\varepsilon_r-1.93)^{0.48\cos\theta}}{\sin^{7.88}\theta\exp\left(2k_z^2\sigma^2\right)}\sum_{n=1}^{\infty}\left[\frac{4175.4\sin^{0.11}(\theta+0.3)\sin^{3.91}(0.1\theta)}{\sin^{0.86}(\theta+1.5)}2^n\exp\left(-2k_z^2\sigma^2\right) - \frac{\sin^{5.9}\theta\sin^{0.22}(\theta+0.5)}{\cos^{3.12}0.8\theta}\right]^2\frac{k_z^{2n}\sigma^{2n}W^n(-2k_x,0)}{n!} \tag{22}$$

$$\sigma^0_{vv} = \frac{53k^2\exp\left(-3.996\sigma^2k_z^2\right)\left[0.5-(\varepsilon_r+3)^{-\cos(1.02\theta-0.2)}\right]^{5.4}\sigma^{-0.05}}{\sin^{3.35}(\theta+1.1)\tan^{-0.46}(\theta+0.32)(L-0.049)^{[0.042+0.06\sin(\theta-1)]}}\sum_{n=1}^{\infty}\frac{(2k_z\sigma)^{2n}W^n(-2k_x,0)}{n!} \tag{23a}$$

$$\sigma^0_{vv} = \frac{k^2\exp\left(-158.14-59.5\sigma-3.8664\sigma^2k_z^2\right)\left[7-(\varepsilon_r+2.2)^{-\cos(0.98\theta-0.2)}\right]^{81.61}}{2\exp\left[-2.31\tan(0.9\theta)\right]\sin^{2.1}(\theta+0.77)(L-0.046)^{[0.08+0.07\sin(\theta-1.7)]}}\sum_{n=1}^{\infty}\frac{(2k_z\sigma)^{2n}W^n(-2k_x,0)}{n!} \tag{23b}$$

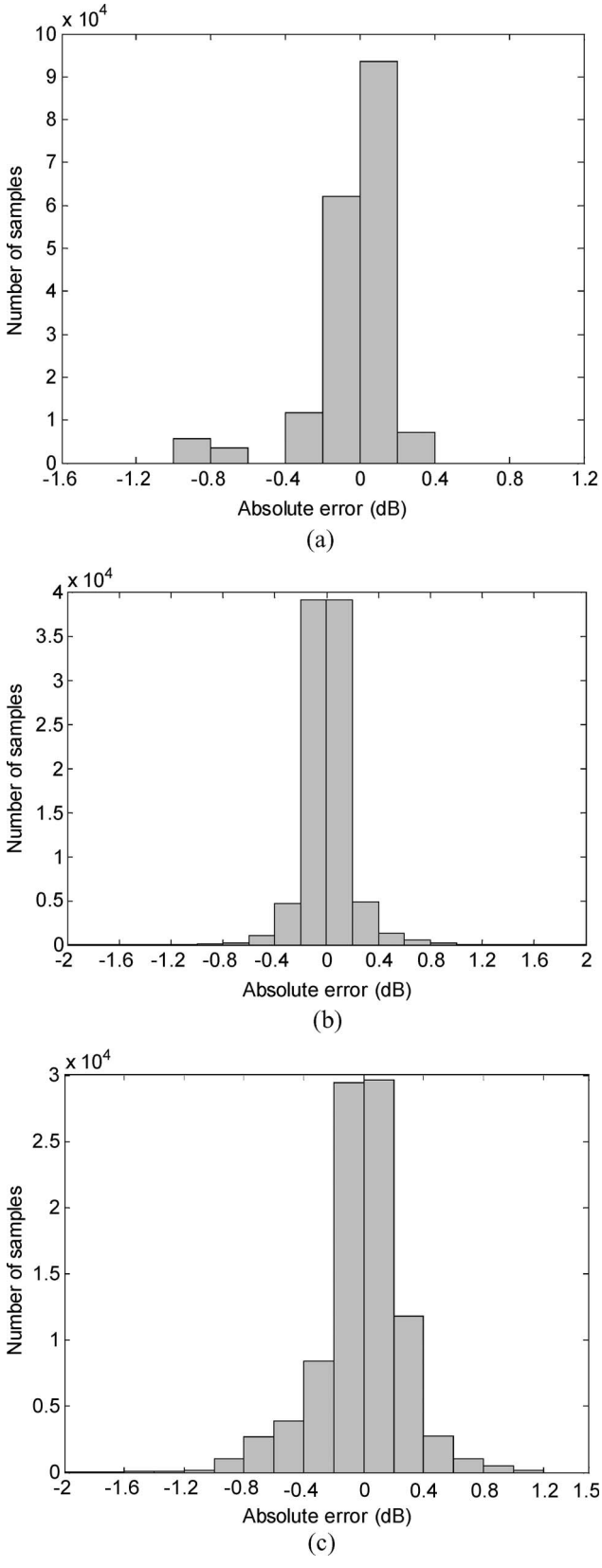

Fig. 2. Histograms of absolute error (in decibels) between the IEM and the EA-IEM for (a) σ^0_{hh}, (b) σ^0_{vv} for the Gaussian surface correlation function, and (c) σ^0_{vv} for the exponential surface correlation function. The total number of computation samples is 183 600 for (a) and 91 800 for (b) and (c).

($\theta > 50^\circ$), small soil dielectric constant ($\varepsilon_r < 7$), and high rms height ($\sigma > 20$ mm). These computation samples that show an error greater than 1 dB account for about 0.6% and 0.4% of all for the Gaussian and exponential surface correlation functions, respectively. For the horizontally copolarized backscattering coefficients σ^0_{hh}, the fit is even better—the absolute difference is less than 1 dB for all 183 600 sample calculations. The fit for the Gaussian surface correlation function is better than that for the exponential surface correlation function for the vertically copolarized backscattering coefficients σ^0_{vv}. These results may indicate that the EA-IEM well represents the original IEM.

Since the IEM is a multiparameter model, we use a case study to illustrate the difference between the EA-IEM and the original IEM. The relationship of the errors with soil roughness or dielectric constant is shown in Fig. 3 for incidence angles of 10°, 35°, and 60°, where the surface correlation function is the exponential function, with the correlation length being 15 cm and the frequency being 5.3 GHz; the error is within 2 dB for the following parameter domain: the dielectric constant from 4 to 42, the rms height from 0.4 cm to 3.1 cm, and the incidence angles of 10°, 35°, and 60°. Outside this parameter domain, the following are observed: 1) the error is not sensitive to the incidence angle; 2) the error increases with decreasing dielectric constant when the dielectric constant is less than seven for HH-polarization; 3) for VV-polarization, the error increases with increasing incidence angle when $\theta > 60^\circ$, with increasing rms height when it is greater than 25 mm, and with decreasing dielectric constant when it is less than seven. For VV-polarization, the error is dependent on the incidence angle, and the error increases at an incidence angle larger than 60°, for an rms height more than 25 mm and a dielectric constant less than seven.

IV. Model Assessment Through Analysis of Calibration Errors of Active Microwave System

The calibration of active microwave instruments also affects the results of the reversion of soil moisture. To assess the sensitivity of the EA-IEM to calibration errors (uncertainties) of active microwave systems in retrieving soil moisture content, a calibration error analysis is performed. Calibration error for either the HH-polarization mode or VV-polarization mode is assumed to include two components: absolute calibration error and relative calibration error. The absolute calibration error (E_a) is defined as the common offset affecting both the horizontally copolarized backscattering coefficient $10\log_{10}(\sigma^0_{hh})$ and the vertically copolarized backscattering coefficient $10\log_{10}(\sigma^0_{vv})$, and the relative calibration error (E_r) is defined as the offset factor in the ratio $10\log_{10}(\sigma^0_{hh}/\sigma^0_{vv})$. Based on these definitions, the calibrated backscattering coefficients ($\overline{\sigma^0_{hh}}$ and $\overline{\sigma^0_{vv}}$) are then expressed in terms of the measured backscattering coefficient and calibration error as follows:

$$10\log_{10}\left(\overline{\sigma^0_{hh}}\right) = E_a + E_{r1} + 10\log_{10}\left(\sigma^0_{hh}\right) \quad (24)$$

$$10\log_{10}\left(\overline{\sigma^0_{vv}}\right) = E_a + E_{r2} + 10\log_{10}\left(\sigma^0_{vv}\right) \quad (25)$$

$$10\log_{10}\left(\frac{\overline{\sigma^0_{hh}}}{\overline{\sigma^0_{vv}}}\right) = E_r + 10\log_{10}\left(\frac{\sigma^0_{hh}}{\sigma^0_{vv}}\right) \quad (26)$$

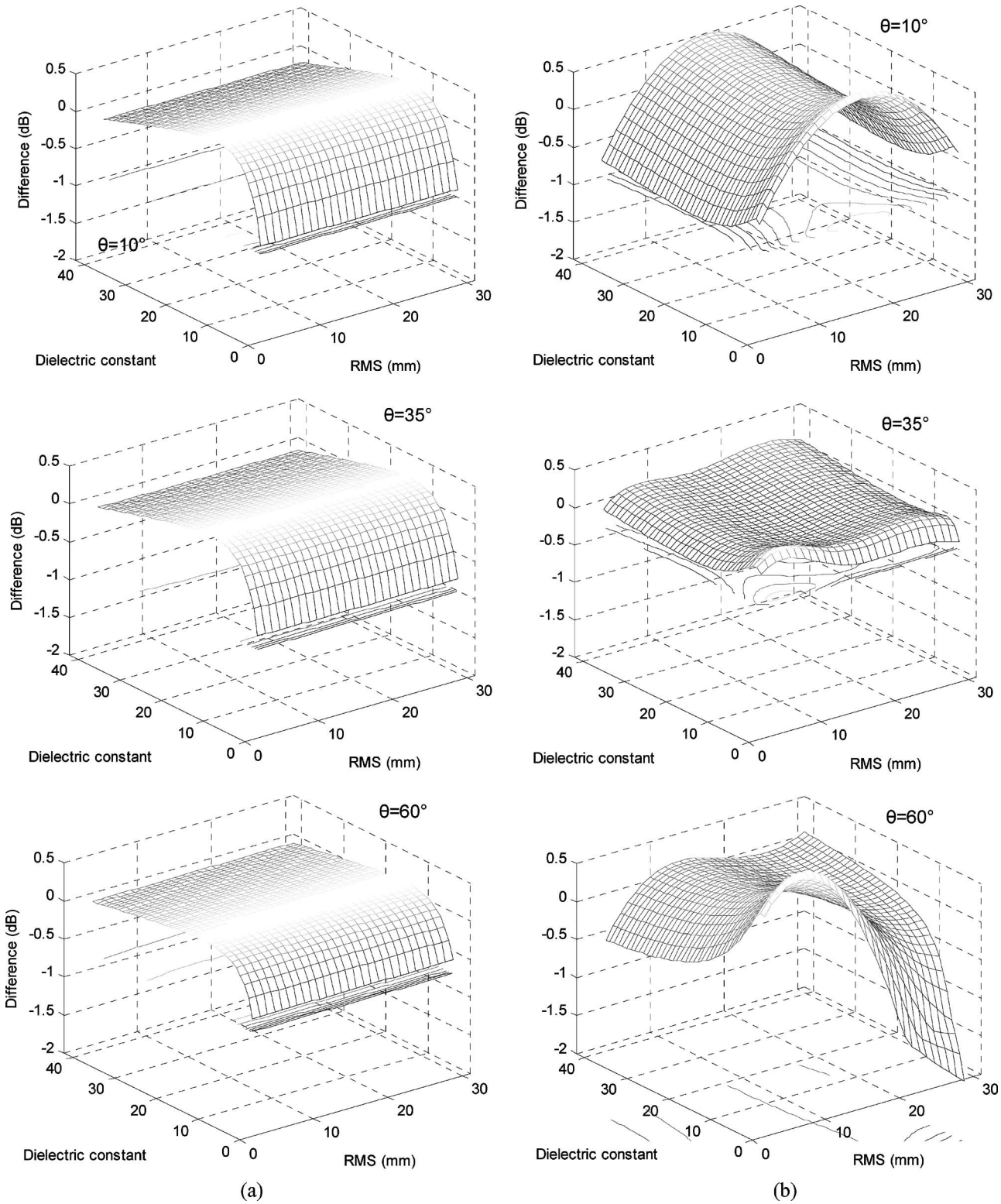

Fig. 3. Differences between the EA-IEM and the original IEM for (a) σ^0_{hh} and (b) σ^0_{vv}. The left panel is for HH-polarization, while the right panel is for VV-polarization.

where E_a is the absolute calibration error and $E_r = E_{r1} - E_{r2}$ is the relative calibration error. Note that all quantities are in decibels. E_a and E_r are determined in the calibration process, according to [14].

Soil dielectric constant can be calculated directly using (15), (20a), and (20b) from the backscattering coefficient. Soil moisture is then inverted using a set of empirical dielectric constant mixing models [24]. Fig. 4 shows errors in soil moisture content estimation from $\overline{\sigma^0_{hh}}$ and $\overline{\sigma^0_{vv}}$ versus absolute calibration error (with $E_{r1} = E_{r2} = 0$) at different incidence angles for horizontal and vertical copolarizations, respectively. Fig. 5 shows the errors in soil moisture content

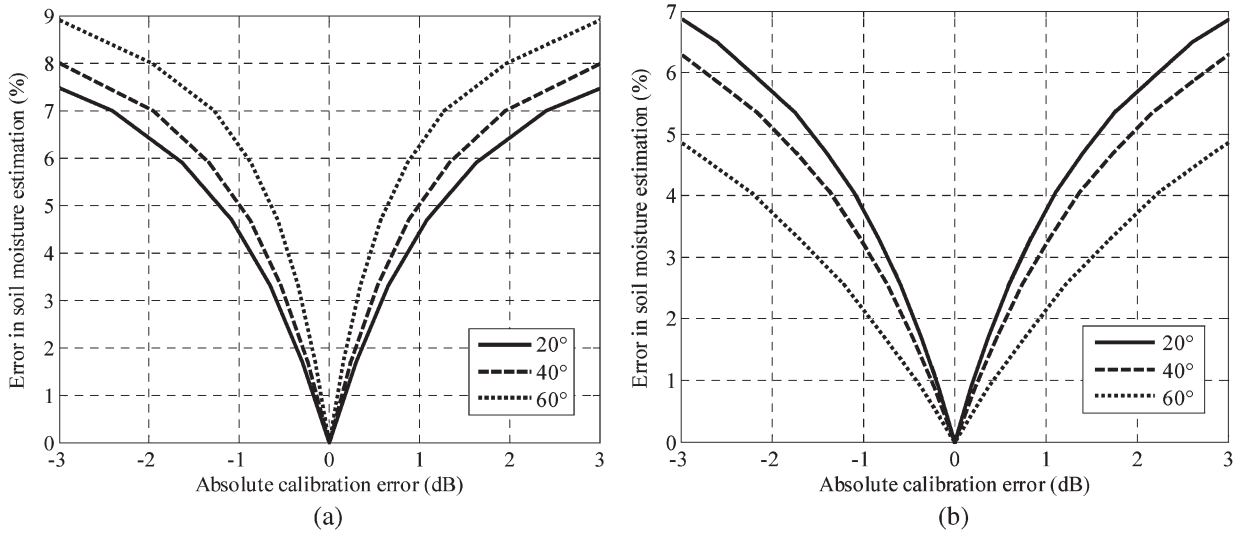

Fig. 4. Sensitivity tests of the EA-IEM in the soil moisture estimation to absolute calibration error. (a) For HH-polarization. (b) For VV-polarization.

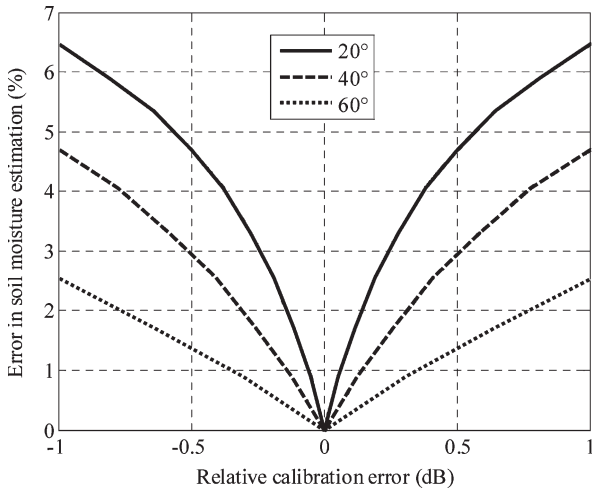

Fig. 5. Sensitivity test of the EA-IEM in the soil moisture estimation to relative calibration error.

estimation versus relative calibration error for different incidence angles.

From Fig. 4, we can see that the inversion of soil moisture from σ^0_{hh} is more sensitive to absolute calibration errors at larger incidence angles, while the inversion of soil moisture from σ^0_{vv} is more sensitive to absolute calibration errors at smaller incidence angles. If the desired accuracy in measurements is about 4%, Fig. 4(a) suggests that the EA-IEM can provide satisfactory soil moisture estimation from measurements of σ^0_{hh}, when absolute calibration errors are within ± 0.5 dB over the range of 20°–60° of incidence angle. Fig. 4(b) suggests that the model can provide satisfactory soil moisture estimation from measurements of σ^0_{vv} when absolute calibration errors are within ± 1 dB over the range of 20°–60° of incidence angle. When absolute calibration errors are estimated to be smaller than 3 dB, the error in the soil moisture estimation from σ^0_{vv} will be less than 5% at 60°, and that from σ^0_{hh} is less than 7.5% at 20°.

Comparing Fig. 4 with Fig. 5, we can see that the EA-IEM is less sensitive to the relative calibration error. From Fig. 5, it can also be seen that the sensitivity of soil moisture to the relative calibration error decreases with increasing incidence angle. The error in the soil moisture estimation is less than 2.6% at 60° with relative calibration errors within ± 1 dB. This may indicate that the EA-IEM is applicable to retrieve the soil moisture at incidence angles as large as 60°.

From these sensitivity studies, we conclude that the inversion of soil moisture using the EA-IEM is more sensitive to absolute calibration errors than relative calibration errors. In order to avoid errors in the soil moisture estimation larger than 5% over the range of 20°–60° of incidence angle, the relative calibration error must be within ± 0.5 dB, and the absolute calibration error should be within ± 1.5 dB for VV-polarization and ± 0.5 dB for HH-polarization. It should be used with caution for the soil moisture estimation from active microwave measurements at incidence angles larger than 60° with absolute calibration errors exceeding ± 2 dB for HH-polarization, and at incidence angles smaller than 20° with absolute calibration errors exceeding ± 3 dB for VV-polarization.

V. Model Assessment Through Comparison With *In Situ* Measurement

The error in the measured backscattering coefficients will propagate into the soil retrieval and thus affect the accuracy of the retrieved soil moisture content. To demonstrate how the error in the backscattering coefficient propagates into the soil moisture retrieval using the EA-IEM, we consider the case that $f = 1.5$ GHz, $\theta = 35°$, $\sigma = 15$ mm, $L = 150$ mm, and the correlation function is the exponential function. Assuming a specific value of the backscattering coefficient (e.g., -18 dB for both HH- and VV-polarizations), the soil moisture is retrieved from the EA-IEM and the dielectric constant mixing model [24]. This case is treated as the accurate case. Now, assume that there is an error in the backscattering coefficient varying from 0 to 2 dB superimposed onto the accurate case, meaning that the backscattering coefficient varies from -18 to -16 dB. For each value of the backscattering coefficient, the soil moisture is then retrieved. After subtracting the soil moisture retrieved

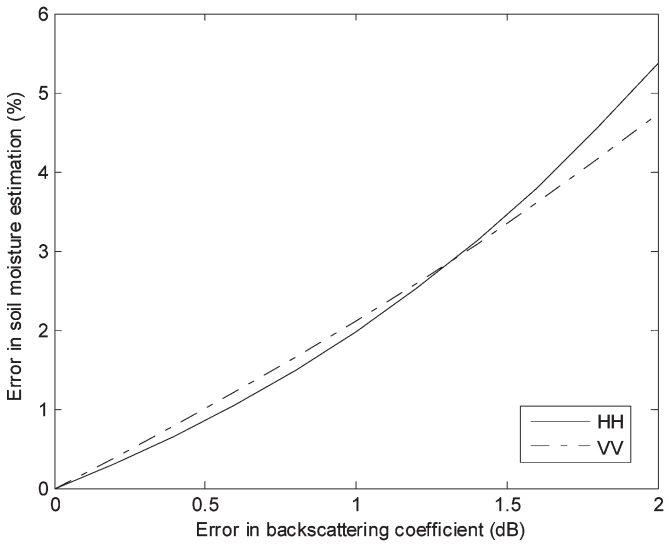

Fig. 6. Error propagation from the backscattering coefficient to the soil moisture estimation for the case that $f = 1.5$ GHz, $\theta = 35^\circ$, $\sigma = 15$ mm, $L = 150$ mm, the correlation function is the exponential function, and the radar backscattering coefficient is -18 dB for both HH- and VV-polarizations.

for the accurate case, we obtain the error in the soil moisture for each error in the backscattering coefficient. The results are shown in Fig. 6. The soil moisture varies from 0% to 5.4% (HH-polarization) or 4.7% (VV-polarization) in volume over the error range of the radar backscattering coefficient. The error in the soil moisture retrieved from the radar backscattering coefficient increases nonlinearly with the error in the radar backscattering coefficient. This example also indicates that the soil moisture retrieved from VV-polarization is less sensitive to the error in the backscattering coefficient than that retrieved from HH-polarization when the error in the radar backscattering coefficient exceeds 1.5 dB.

From the previous error analyses, we found the following: 1) The error in the soil moisture retrieval using the EA-IEM increases monotonically with the error in the backscattering coefficient, and 2) the error in the backscattering coefficient calculated from the EA-IEM as compared with the original IEM is within certain parameter domains (Fig. 3).

Comparison with *in situ* measurements is the best way for model assessment. However, simultaneous *in situ* measurements of both radar backscattering coefficients and soil surface conditions are scarce due to the sophistication of the active microwave system and difficulty in soil surface characterization. We use the limited data sets available in the literature for this task.

The first set of data is from Fung *et al.* [17]. We use the data of Fung *et al.* to demonstrate the predictability of dependence of the backscattering coefficient on the incident angle by both the original IEM and the EA-IEM. Comparisons between the measured and the computed backscattering coefficients using the original IEM and the EA-IEM over the incident angle range from 10° to 70° at two frequencies of 4.725 and 9.525 GHz are shown in Figs. 7 and 8. In Fig. 7, the rms height is 0.4 cm, the correlation length is 8.4 cm, and the soil surface moisture content is 14%, corresponding to a soil dielectric constant of about 7.5 [24]–[26]. In Fig. 8, the rms height is 0.32 cm, the correlation length is 9.9 cm, and the soil surface moisture content is 30%, corresponding to a soil dielectric constant of about 16. From Figs. 7 and 8, it can be seen that the computed results using the EA-IEM agree well with the original IEM and that the error between them is less than 1 dB. Also, it is noted that the difference between the modeling results and the measured values was found to become larger when the incidence angle increases. For VV-polarization, the difference is smaller than 5 dB for the whole range of θ (10°–70°) and becomes larger at higher frequency. On the other hand, the difference is almost more than 5 dB over the incidence angle of 50°–70° for HH-polarization, particularly at higher frequency. Overall, good agreements are seen between the EA-IEM and measurements for copolarizations, specifically VV-polarization.

The other *in situ* data sets are from Oh *et al.* [15], [27] and Neusch and Sties [28] over various soil surfaces with different roughness and wetness conditions. The measured data from [15], [19], and [27] were used to demonstrate the predicative power of the original IEM and the EA-IEM for the soil moisture retrieval. Comparisons of the soil moisture content derived by the original IEM and the EA-IEM and the measurements are shown in Fig. 9. For the data set of Oh *et al.*, the soil surface roughness parameters and the surface soil moisture are shown in Table II. The range of $k\sigma$ varies from 0.1 to 3, whereas kL varies from 2.4 to 9.8, which fall in the applicable region of the model (see Table I). The exponential correlation function was found to fit the first three surface profiles, and the Gaussian correlation function was found to fit the roughest field profile (S-4, see Table II). The data inversions include two frequencies (1.5 and 4.75 GHz), and the incidence angles vary from 10° to 60°. For the data set of Oh *et al.*, the soil surface roughness parameters and the surface soil moisture are shown in Table III, and the incidence angle is about 55°. Table IV shows the soil surface roughness parameters and the surface soil moisture of the data set of Neusch *et al.*, and the incidence angle is about 55°. The volumetric soil moisture is used in this investigation. The other parameters can be found in the literature [27], [28]. When the original IEM and the EA-IEM are used to predict the soil moisture values measured by Oh *et al.* and and Neusch *et al.*, the rms deviations (rmsd) are 3.69% and 3.64% in volume for the IEM and the EA-IEM, respectively. Linear regression analysis between the model prediction and measurement shows that the coefficients of determination (R^2) are 0.68 and 0.70 for the IEM and the EA-IEM, respectively. Both rmsd and R^2 show that the EA-IEM is slightly better than the original IEM in predicting the measurement. However, the overall similarity in the predictive power (rmsd) and coefficient of determination (R^2) between the IEM and the EA-IEM indicates again that the EA-IEM represents well the original IEM.

It can be seen from the comparison shown in Fig. 9 that the rms error between the measured data and the soil moisture content derived by the EA-IEM indicates that the soil moisture can be estimated with an average error of less than 3.4%, and the soil moisture content derived by the EA-IEM is almost the same as that derived by the original IEM. A very good agreement between the EA-IEM results and the measured data

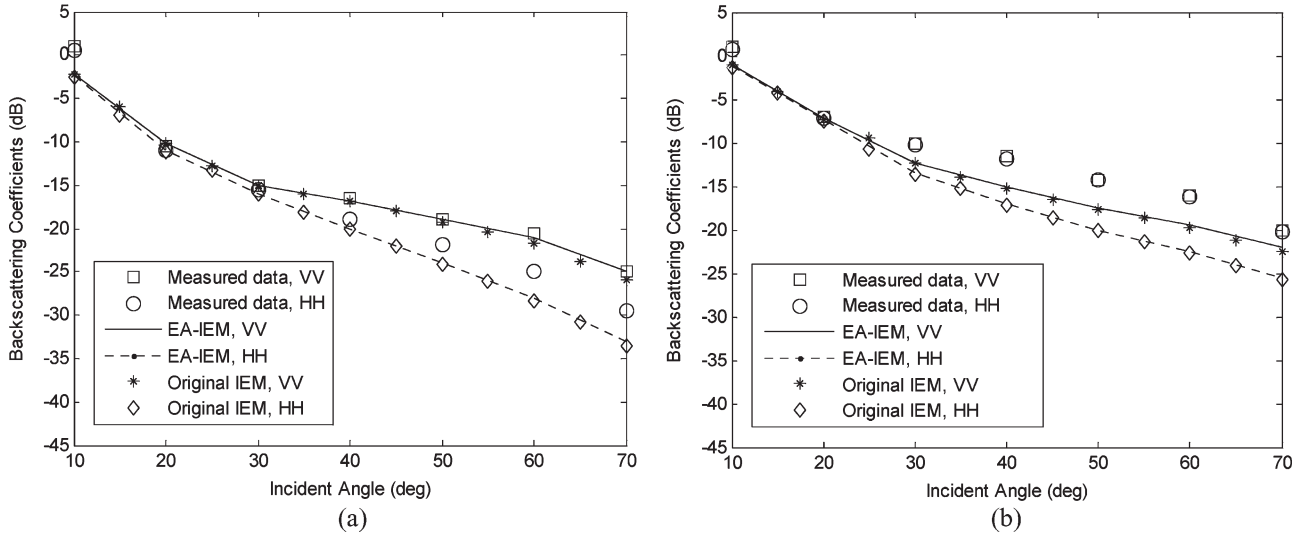

Fig. 7. Comparisons of (lines) the model predictions with (symbols) the measurements at (a) 4.725 GHz and (b) 9.525 GHz.

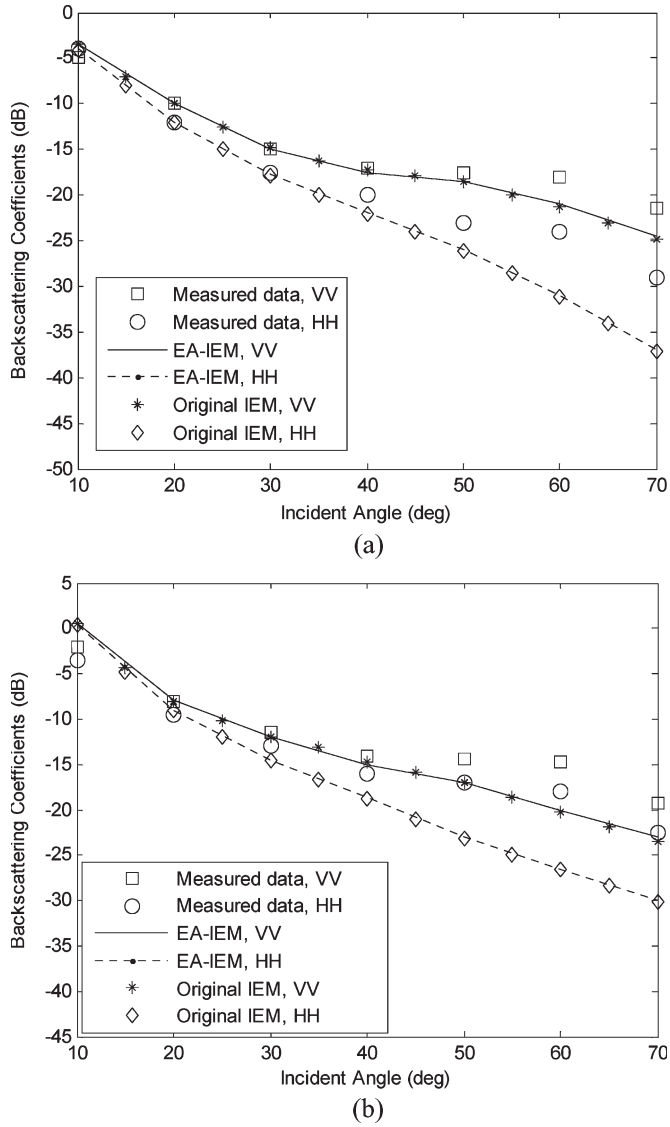

Fig. 8. Comparisons of (lines) the model predictions with (symbols) the measurements at (a) 4.725 GHz and (b) 9.525 GHz.

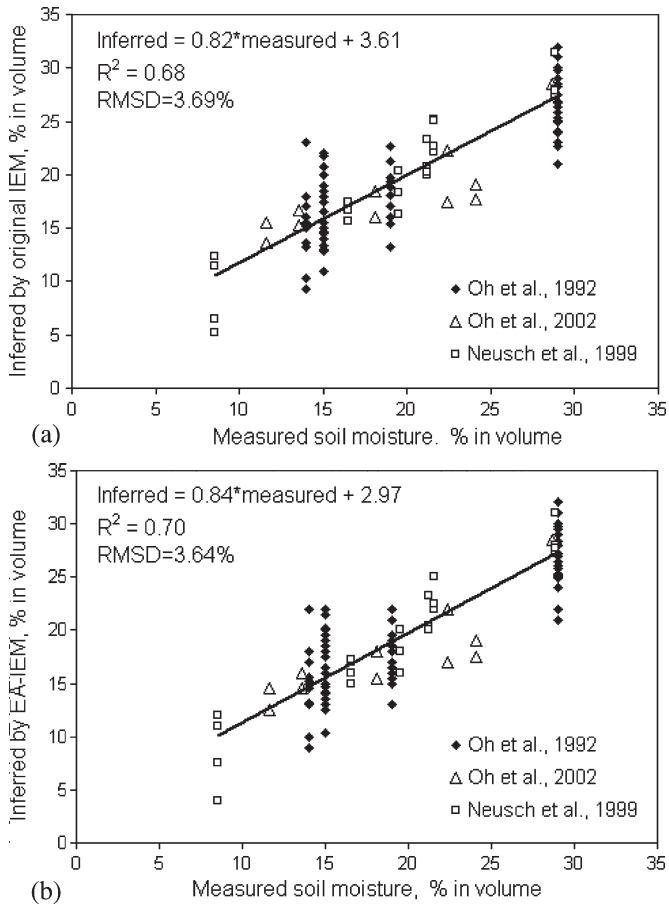

Fig. 9. Comparisons of the soil moisture content inverted from the original IEM and the EA-IEM with the measurements by Oh *et al.* [15], [27] and Neusch and Sties [28]. (a) Inverted from the original IEM. (b) Inverted from the EA-IEM.

is observed. However, for small incidence angle $(\theta \leq 10^\circ)$ and large incidence angle $(\theta \geq 60^\circ)$, larger errors can occur. Additional experimental measurements over a wider range of roughness and moisture conditions are obviously desired for further model assessment.

TABLE II
SOIL ROUGHNESS AND MOISTURE PARAMETERS

Surface	σ (mm)	L (mm)	Freq (GHz)	kσ	kL	soil moisture
S-1	4	84	1.50	0.13	2.6	29%
S-1	4	84	1.50	0.13	2.6	15%
S-1	4	84	4.75	0.40	8.4	29%
S-1	4	84	4.75	0.40	8.4	15%
S-2	3.2	99	1.50	0.10	3.1	15%
S-2	3.2	99	1.50	0.10	3.1	14%
S-2	3.2	99	4.75	0.32	9.8	15%
S-2	3.2	99	4.75	0.32	9.8	14%
S-3	11.2	84	1.50	0.35	2.6	15%
S-3	11.2	84	4.75	1.11	8.4	15%
S-4	30.2	88	1.50	0.95	2.8	19%
S-4	30.2	88	1.50	0.95	2.8	15%
S-4	30.2	88	4.75	3.00	8.8	19%
S-4	30.2	88	4.75	3.00	8.8	15%

TABLE III
SOIL ROUGHNESS AND MOISTURE PARAMETERS

σ (mm)	L (mm)	soil moisture
18.2	177.5	28.7%
18.2	177.5	24.1%
18.2	177.5	22.4%
18.2	177.5	18.1%
18.2	177.5	13.6%
18.2	177.5	11.6%

TABLE IV
SOIL ROUGHNESS AND MOISTURE PARAMETERS

σ (mm)	L (mm)	soil moisture
17	56	28.85%
17.8	56	21.57%
14.9	50	21.2%
15.6	52	19.53%
14.5	50	16.52%
18.9	58	8.53%

VI. CONCLUSION

Model complexity and the implicit relationship between active microwave backscattering coefficient and soil dielectric constant make the retrieval of soil moisture using the IEM unnecessarily complicated and nonparsimonious in computation, particularly when it is used to retrieve soil moisture from high-resolution active microwave backscattering coefficient data. To invert the soil moisture directly from the backscattering coefficient measurements using the IEM, we empirically adopted the model and tested the fit of the EA-IEM to the original IEM under a wide range of soil dielectric constant, incidence angle, rms height, and surface correlation length. We adopted the schedules as described in this paper to obtain the soil dielectric constant as an analytical function of backscattering coefficient, rather than the other way around, just as the case of the original IEM. Thus, the contribution of this paper is that the EA-IEM expresses the soil dielectric constant and, thus, soil moisture as an explicit analytic function of active microwave backscattering coefficient. Therefore, the inversion of soil moisture from the active microwave backscattering coefficient becomes direct and computationally efficient.

The absolute errors of backscattering coefficients between the EA-IEM and the original IEM have also been analyzed. For horizontal polarization, all of the errors are less than 1 dB, while some of the errors are larger than 1 dB at small soil dielectric constants ($\varepsilon_r < 7$) and high rms height ($\sigma > 20$ mm) for vertical polarization. In addition, the average error of backscattering coefficients for the HH-polarization mode is 0.14 dB, while the average errors for VV-polarization mode are 0.12 and 0.2 dB, corresponding to the Gaussian and exponential surface correlation functions, respectively.

We also quantified the calibration requirements of the inversion model developed. If soil moisture must be retrieved at an accuracy better than 5% over the range of 20°–60°, the active microwave data must be calibrated to within 1.5-dB absolute value for σ^0_{vv}, 0.5-dB absolute value for σ^0_{hh}, and 0.5-dB relative value. The EA-IEM, in combination with soil dielectric constant mixing models, has been used to derive the soil moisture from the *in situ* backscattering coefficient measurements in the literature [15], [17], [27], [28]. The retrieved values are then compared with the *in situ* measurement of soil moisture. It is found that the soil moisture derived from the EA-IEM agrees with the *in situ* measurement within an average accuracy of 3.4% for both copolarizations, particularly VV-polarization. All the model assessments (model intercomparison, error analysis, and comparison with *in situ* measurement) indicate that the EA-IEM is a good representative of the original IEM and can be used to retrieve soil moisture under the tested range of model parameters: incidence angles between 10° and 60°, soil dielectric constants between 4 and 42, surface rms height between 4 and 31 mm, surface correlation length between 50 and 250 mm, and other surface parameters that are same as those of the original IEM. The advantage is that the inversion of soil moisture from active microwave measurements using the EA-IEM is now direct and computationally efficient.

REFERENCES

[1] C. Notarnicola, M. Angiulli, and F. Posa, "Soil moisture retrieval from remotely sensed data: Neural network approach versus Bayesian method," *IEEE Trans. Geosci. Remote Sens.*, vol. 46, no. 2, pp. 547–557, Feb. 2008.

[2] M. Zribi, C. André, and B. Decharme, "A method for soil moisture estimation in western Africa based on the ERS scatterometer," *IEEE Trans. Geosci. Remote Sens.*, vol. 46, no. 2, pp. 438–448, Feb. 2008.

[3] M. Moghaddam, Y. Rahmat-Samii, E. Rodriguez, D. Entekhabi, J. Hoffman, D. Moller, L. E. Pierce, S. Saatchi, and M. Thomson, "Microwave observatory of subcanopy and subsurface (MOSS): A mission concept for global deep soil moisture observations," *IEEE Trans. Geosci. Remote Sens.*, vol. 45, no. 8, pp. 2630–2643, Aug. 2007.

[4] C.-H. Kuo and M. Moghaddam, "Electromagnetic scattering from multilayer rough surfaces with arbitrary dielectric profiles for remote sensing of subsurface soil moisture," *IEEE Trans. Geosci. Remote Sens.*, vol. 45, no. 2, pp. 349–366, Feb. 2007.

[5] S. C. Dunne, D. Entekhabi, and E. G. Njoku, "Impact of multiresolution active and passive microwave measurements on soil moisture estimation using the ensemble Kalman smoother," *IEEE Trans. Geosci. Remote Sens.*, vol. 45, no. 4, pp. 1016–1028, Apr. 2007.
[6] N. E. C. Verhoest, B. de Baets, and H. Vernieuwe, "A Takagi-Sugeno fuzzy rule-based model for soil moisture retrieval from SAR under soil roughness uncertainty," *IEEE Trans. Geosci. Remote Sens.*, vol. 45, no. 5, pp. 1351–1360, May 2007.
[7] A. Loew, R. Ludwig, and W. Mauser, "Derivation of surface soil moisture from ENVISAT ASAR wide swath and image mode data in agricultural areas," *IEEE Trans. Geosci. Remote Sens.*, vol. 44, no. 4, pp. 889–899, Apr. 2006.
[8] J. Álvarez-Mozos, J. Casalí, M. González-Audícana, and N. E. C. Verhoest, "Assessment of the operational applicability of RADARSAT-1 data for surface soil moisture estimation," *IEEE Trans. Geosci. Remote Sens.*, vol. 44, no. 4, pp. 913–924, Apr. 2006.
[9] U. Narayan, V. Lakshmi, and T. J. Jackson, "High-resolution change estimation of soil moisture using L-band radiometer and radar observations made during the SMEX02 experiments," *IEEE Trans. Geosci. Remote Sens.*, vol. 44, no. 6, pp. 1545–1554, Jun. 2006.
[10] J. D. Bolten, V. Lakshmi, and E. G. Njoku, "Soil moisture retrieval using the passive/active L- and S-band radar/radiometer," *IEEE Trans. Geosci. Remote Sens.*, vol. 41, no. 12, pp. 2792–2801, Dec. 2003.
[11] E. S. Kasischke, L. L. Bourgeau-Chavez, and J. F. Johnstone, "Assessing spatial and temporal variations in surface soil moisture in fire-disturbed black spruce forests in Interior Alaska using spaceborne synthetic aperture radar imagery—Implications for post-fire tree recruitment," *Remote Sens. Environ.*, vol. 108, no. 1, pp. 42–58, May 2007.
[12] E. E. Sano, M. S. Moran, A. R. Huete, and T. Miura, "C- and multiangle Ku-band synthetic aperture radar data for bare soil moisture estimation in agricultural areas," *Remote Sens. Environ.*, vol. 64, no. 1, pp. 77–90, Apr. 1998.
[13] M. Zribi and M. Dechambre, "A new empirical model to retrieve soil moisture and roughness from C-band radar data," *Remote Sens. Environ.*, vol. 84, no. 1, pp. 42–52, Jan. 2003.
[14] P. C. Dubois, J. V. Zyl, and T. Engman, "Measuring soil moisture with imaging radars," *IEEE Trans. Geosci. Remote Sens.*, vol. 33, no. 4, pp. 915–926, Jul. 1995.
[15] Y. Oh, K. Sarabandi, and F. T. Ulaby, "An empirical model and an inversion technique for radar scattering from bare soil surface," *IEEE Trans. Geosci. Remote Sens.*, vol. 30, no. 2, pp. 370–381, Mar. 1992.
[16] J. Shi, J. Wang, A. Y. Hsu, P. E. O'Neill, and E. T. Engman, "Estimation of bare surface soil moisture and surface roughness parameter using L-band SAR image data," *IEEE Trans. Geosci. Remote Sens.*, vol. 35, no. 5, pp. 1254–1266, Sep. 1997.
[17] A. K. Fung, Z. Li, and K. S. Chen, "Backscattering from a randomly rough dielectric surface," *IEEE Trans. Geosci. Remote Sens.*, vol. 30, no. 2, pp. 356–369, Mar. 1992.
[18] K. S. Chen, S. K. Yen, and W. P. Huang, "A simple model for retrieving bare soil moisture from radar-scattering coefficients," *Remote Sens. Environ.*, vol. 54, no. 2, pp. 121–126, Nov. 1995.
[19] F. T. Ulaby, R. K. Moore, and A. K. Fung, *Microwave Remote Sensing: Active and Passive*, vol. II. Reading, MA: Addison-Wesley, 1982.
[20] Y. Oh and Y. C. Kay, "Condition for precise measurement of soil surface roughness," *IEEE Trans. Geosci. Remote Sens.*, vol. 36, no. 2, pp. 691–695, Mar. 1998.
[21] M. W. J. Davidson, T. Le Toan, F. Mattia, G. Satalino, T. Manninen, and M. Borgeaud, "On the characterization of agricultural soil roughness for radar remote sensing studies," *IEEE Trans. Geosci. Remote Sens.*, vol. 38, no. 2, pp. 630–640, Mar. 2000.
[22] F. Mattia, M. W. J. Davidson, T. Le Toan, C. M. F. D'Haese, N. E. C. Verhoest, A. M. Gatti, and M. A. Borgeaud, "A comparison between soil roughness statistics used in surface scattering models derived from mechanical and laser profilers," *IEEE Trans. Geosci. Remote Sens.*, vol. 41, no. 7, pp. 1659–1671, Jul. 2003.
[23] M. Callens, N. E. C. Verhoest, and M. W. J. Davidson, "Parameterization of tillage-induced single-scale soil roughness from 4-m profiles," *IEEE Trans. Geosci. Remote Sens.*, vol. 44, no. 4, pp. 878–888, Apr. 2006.
[24] M. T. Hallikainen, F. T. Ulaby, M. C. Dobson, M. A. El-Rayes, and L. Wu, "Microwave dielectric behavior of wet soil—Part I: Empirical models and experimental observations," *IEEE Trans. Geosci. Remote Sens.*, vol. GRS-23, no. 1, pp. 25–34, Jan. 1985.
[25] G. C. Topp and J. L. Davis, "Measurement of soil water content using time-domain reflectrometry (TDR): A field evaluation," *Soil Sci. Soc. Amer. J.*, vol. 49, no. 1, pp. 19–24, Jan. 1985.
[26] G. C. Topp, J. L. Davis, and A. P. Annan, "Electromagnetic determination of soil water content: Measurements in coaxial transmission lines," *Water Resour. Res.*, vol. 16, no. 3, pp. 574–582, 1980.
[27] Y. Oh, K. Sarabandi, and F. T. Ulaby, "Semi-empirical model of the ensemble-averaged differential Mueller matrix for microwave backscattering from bare soil surfaces," *IEEE Trans. Geosci. Remote Sens.*, vol. 40, no. 6, pp. 1348–1355, Jun. 2002.
[28] T. Neusch and M. Sties, "Application of the Dubois-model using experimental synthetic aperture radar data for the determination of soil moisture and surface roughness," *ISPRS J. Photogramm. Remote Sens.*, vol. 54, no. 4, pp. 273–278, Sep. 1999.

Kaijun Song received the M.S. degree in radio physics and the Ph.D. degree in electromagnetic field and microwave technology from the University of Electronic Science and Technology of China (UESTC), Chengdu, China, in 2005 and 2007, respectively.

He has been with the School of Electronic Engineering, UESTC, since 2007, where he is currently an Associate Professor. From August 2007 to July 2008, he was a Postdoctoral Research Fellow with the Montana Tech of the University of Montana, Butte, on microwave remote sensing technology and microwave circuits. His current research fields include microwave remote sensing theory, modeling, and algorithms; applications in geoscience, geophysics, geology, hydrology, and environmental sciences; electromagnetic theory; and microwave and millimeter-wave devices, circuits, and systems.

Xiaobing Zhou received the B.S. degree in physics from Hunan Normal University, Changsha, China, in 1986, the M.S. degree in theoretical physics from Sichuan University, Chengdu, China, in 1989, and the Ph.D. degree in geophysics, with specialization in remote sensing, from the University of Alaska, Fairbanks, in 2002.

He was with the Southwestern Institute of Physics, Chengdu, as a Research Assistant Professor from 1989 to 1997 and a Research Associate Professor from 1995 to 1997; with the University of California, San Diego, as a Visiting Scientist in 1997; with the Institute of Geophysics, University of Alaska, as a Visiting Scientist in 1998; with New Mexico Tech, Socorro, as a Research Assistant Professor in hydrology from 2002 to 2005; and has been with the Department of Geophysical Engineering, Montana Tech, University of Montana, Butte, as an Assistant Professor in geophysics since 2005. His current research interests include remote sensing theories, algorithm development, and instrumentation (optical remote sensing and imaging radar), data collection and analysis, and applications in earth and environmental sciences, including geophysical exploration.

Yong Fan (M'06) received the B.E. degree from the Nanjing University of Science and Technology, Nanjing, China, in 1985 and the M.S. degree from the University of Electronic Science and Technology of China, Chengdu, China, in 1992.

He is currently with the School of Electronic Engineering, University of Electronic Science and Technology of China. From 1985 to 1989, he was interested in microwave integrated circuits. He has authored or coauthored over 90 papers, 30 of which are searched by SCI and EI. Since 1989, his research interests has been including millimeter-wave communication, electromagnetic theory, millimeter-wave technology, and millimeter-wave systems.

Mr. Fan is a Senior Member of the Chinese Institute of Electronics.